

DEPOSIT CHARACTERIZATION OF A DIESEL ENGINE COMBUSTION CHAMBER BY DROPLETS AT HOT CHAMBER TEMPERATURE: EFFECT OF TEMPERATURE ON EVAPORATION TIME AND DEPOSIT STRUCTURE

Muhammad Taufiq Suryantoro^{1*}, Bambang Sugiarto¹, Danniell Chistian¹, Bintang Samudra¹,
Zofarizal Gusfa¹

¹*Department of Mechanical Engineering, Faculty of Engineering, Universitas Indonesia, Kampus UI Depok, Depok 16424, Indonesia*

(Received: November 2016 / Revised: December 2016 / Accepted: December 2016)

ABSTRACT

In 2016, the mandatory use of biodiesel as a substitute fuel by up to 20%, as introduced by the Indonesian Ministry of Energy and Mineral Resources, forced vehicle manufacturers to invent suitable engines that would accept biodiesel. The use of biodiesel in such a large proportion is highly risky, particularly due to the formation of deposits in the combustion chamber engines. The previous method of fuel droplets are placed on a hot plate approach produces deposits are slightly different from those generated by a real engine, therefore to obtain realistic deposits it is necessary to modify this method so temperatures as hot as those in a real engine. In this study, the potential deposit formation of biodiesel fuel was examined by conducting the deposition process and the evaporation of fuel on a stainless-steel plate (SS), which was placed in a closed space. Deposit characterization was carried out on a hot plate using Scanning Electron Microscopy (SEM). The test results showed differences in the structures of the deposits produced by biodiesel and diesel fuel; fine structures were seen in the former, while those of the latter were rougher and more porous. Deposit results that are similar to what is seen in a real engine will be very helpful for knowing the patterns, structures, and mechanism of the formation of deposits in such an environment.

Keywords: Antioxidants; Biodiesel; Deposits; Structure; Test rig

1. INTRODUCTION

At present, petroleum fuels remain the main propellant for automobiles, ships, and aircraft; unfortunately, such fuels are natural resources that cannot be renewed. For this reason, Indonesia can no longer rely on fossil fuels. That country is rich in natural resources, including vegetables, which have the potential to be used as alternative sources of power. These abundant resources will go to waste if they are not used to eliminate the dependence on fossil fuels.

In 2016, the Indonesian Ministry of Energy and Mineral Resources (ESDM) encouraged the use of defined biodiesel-related policies. Blend 20% biodiesel in diesel fuel known as B20 should begin to be used as a fuel; it seems certain that this development will encourage the automotive industry to develop a diesel engine that able to consume B20. However, this introduces another problem, because a high percentage of biodiesel will cause the growth of deposits inside the internal combustion chamber; a solution to this issue is yet to be found. Accordingly, a comprehensive study is needed to identify how best to address the dilemma. This paper

*Corresponding author's email: taufiq_suryo@yahoo.co.id, Tel. +021-7270032, Fax. +62-21-7270033
Permalink/DOI: <https://doi.org/10.14716/ijtech.v7i8.6936>

describes just such a study.

The experiment comprised a repeated fuel evaporation process on a plate that was placed in a heated room. The standard and quality of biodiesel as an alternative fuel in Indonesia is regulated by the Decree of the Director General of Renewable Energy and Energy Conservation (DJ ETBKE) No. 723 K/10/DJE/ 2013, which refers to the ISO 7182:2012. This method was used to overcome the complexity of the test deposits in the engine and to conserve time, fuel, and the cost of testing. Such a technique has also been deployed by other researchers (Arafin et al., 2008; Arafin et al., 2010). However, in those studies, the test rig used an open system; or in other words, only the plates were heated. In the present study, the hot plate was placed in an enclosed space so that it and the room temperature could be homogeneous while the pressure remained constant. This set-up was sufficiently close to real conditions; in other words, the hot plate was analogous to the engine’s surface components in a closed environment. The idea was to answer the question of how growths could be deposited at both low and high temperatures.

2. EXPERIMENTAL SETUP

2.1. Fuel Testing Method

The diesel fuel used was Pertamina B0, while the biodiesel fuel deployed was B100 FAME.. The biodiesel can be seen in Appendix I.

The test was conducted by putting droplets on a plate, which was then placed inside a hot chamber. The temperature of the chamber was assumed, as combustion chamber diesel engines’ temperatures can be varied as needed. The hot plate used was of AISI 304 material, with dimensions of 0.8 mm × 100 mm × 100 mm (length × width × thickness).

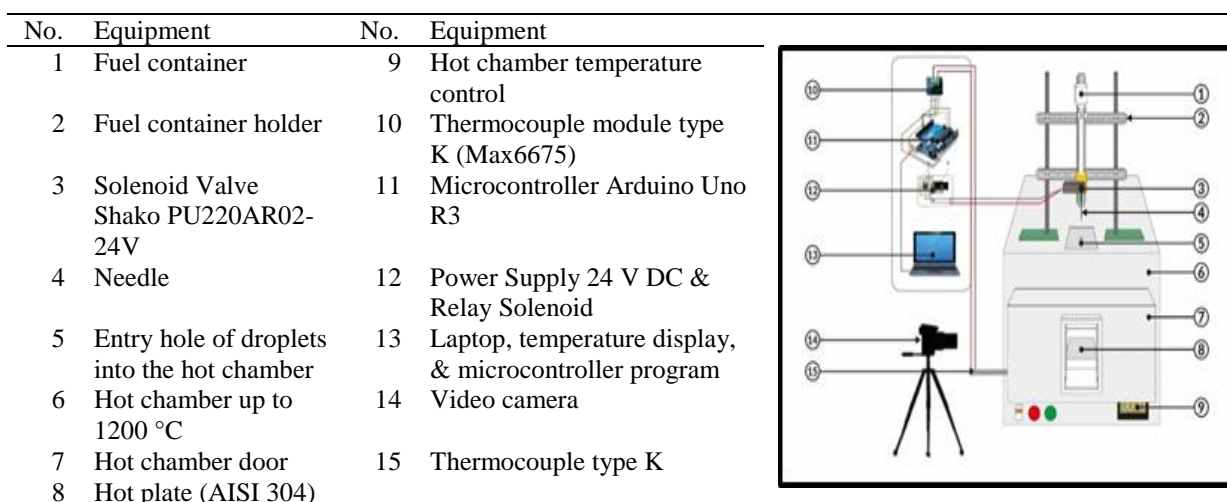


Figure 1 Test equipment for hot chamber surface temperature test rig

2.1.1. Evaporation process for single droplet

The evaporation test was key for obtaining the evaporation characteristic of each type of fuel. In this process, a hot plate, inside a hot chamber temperature deposition test rig, was impinged by fuel. This procedure was conducted twice for each temperature. The fuel evaporation process was recorded using a video camera, from the time a droplet was released from the needle until the fuel was completely evaporated.

2.1.2. Deposition process for multi-droplet

In this process, the tested fuel was dropped continuously at intervals of three seconds onto a hot plate that had been conditioned in the hot chamber temperature test rig. For each temperature, the fuel was dropped up to 10,000 times, with weighing being conducted every 2,000 drops.

The mass of each drop was measured using a density meter. To reduce uncertainty, one drop of fuel mass was calculated by the volume of 100 drops.

After the plate was inserted into the hot chamber, the latter was set to the required temperature, before being kept stable for 10 seconds. This was to ensure that the temperature of the hot plate was equal to that of the chamber.

2.2. Fuel Properties Measurement

Measurement of the fuel’s density and viscosity was performed using the Anton Paar SVM 3000 Stabinger Viscometer. Mass measurements were done with digital analytical scales (ADAM PW 254). The surface deposit contour was observed using a digital microscope KH-8700 HIROX series, while the deposits’ structure was examined via Scanning Electron Microscopy (SEM). Tests were conducted in the Metallurgy and Materials Engineering (DTMM) Department Laboratory, Faculty of Engineering, University of Indonesia.

3. RESULTS AND DISCUSSION

3.1. Evaporation Test Results

The B0 evaporation time at a temperature of 260°C was 6.02 seconds, while for B100 it was 40.63 seconds. Meanwhile, the B0 evaporation time at 300°C was 4.2 seconds, while that of B100 was 24.7 seconds; for both these temperatures, B100 took longer than B0 to evaporate completely (Figure 2).

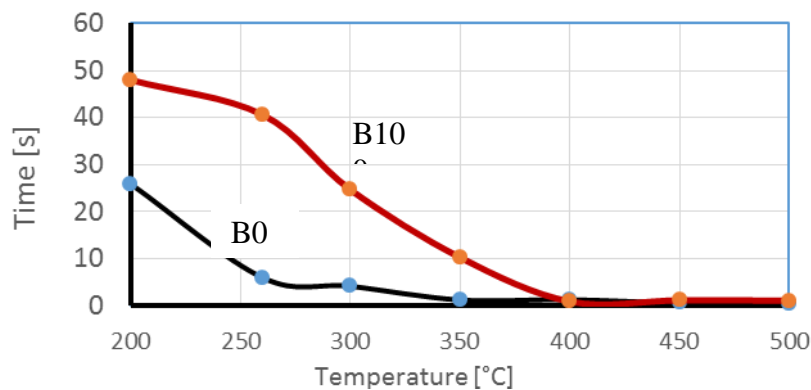


Figure 2 Evaporation time for single droplets of B0 and B100 as chamber temperature function

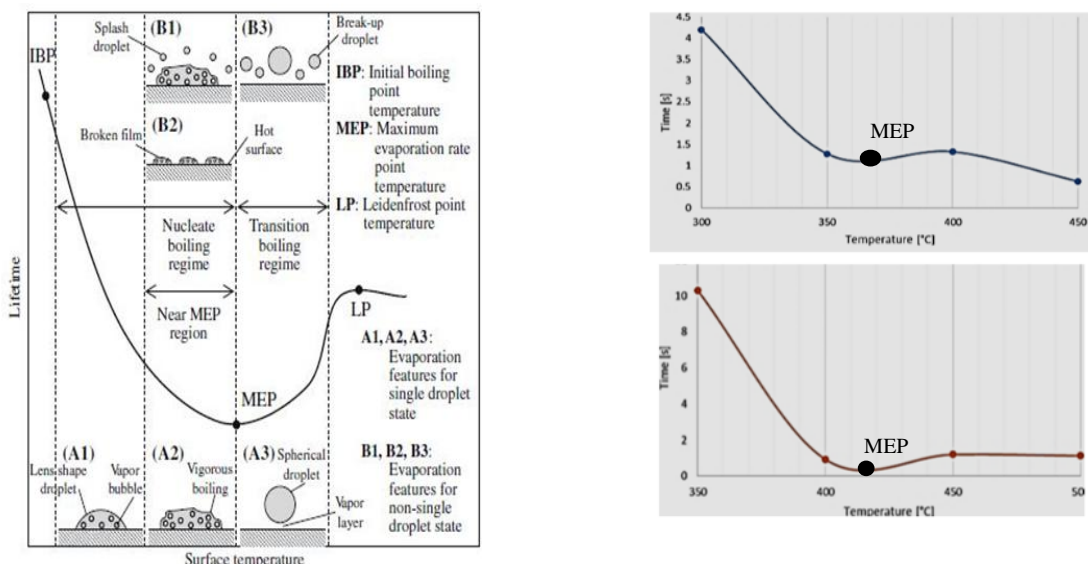


Figure 3 General evaporation characteristics (left). Evaporation characteristic of the fuel droplet of B0 (top right) and B100 (bottom right)

The data clearly showed the evaporation time differences between the two fuels. The transition boiling regime for B0 and B100 started at a temperature of 350°C and ended under temperatures of 500°C for B0 and 450°C for B100. B0 began to burn at temperatures of 500°C, while the B100 did so at 450°C. B100 had a lower auto-ignition point than B0, which shows that it has a higher cetane number.

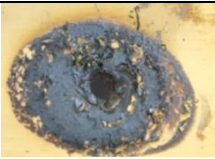

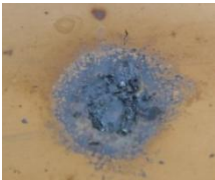
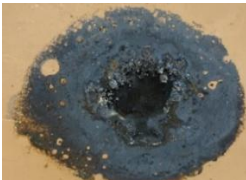
As shown in Figure 3, the maximum evaporation rate point (MEP) temperature of B0 was around 360°C, while that of B100 was around 410°C. Therefore, MEP occurred earlier for the former than for the latter.

3.2. Antimicrobial Activity of Synthetic Organophosphorus Compounds

3.2.1. Deposit mass

Table 1 shows that the deposit attached to the plate was a function of temperature and fuel. At a temperature of 260°C, there were great differences between B0 and B100. However, if the temperature was increased from 260 to 300°C, the deposit mass reduction looked very different. The reduction of B0's mass was very significant, at about 7×, while this was only 1.7× for B100.

Table 1 Deposit mass produced from the multi-droplet deposition of 10,000 drops

Temperature (°C)	Fuel	
	B0	B100
260	 mass: 119.7 mg	 mass: 190.3 mg
300	 mass: 16.4 mg	 mass: 109.1 mg

At 260°C, the deposit character of B0 was slightly dry, while B100 deposits tended to be wet. At 300°C, B0 deposits tended to be dry while deposits of B100 still had wet portions.

3.2.2. Shape of surface and deposits structure

The Figure 4 shows surface shape of both fuels, at a temperature of 260°C, was similar. Near to the surface, the core droplet was seen to be rough; however, B0 tended to be corrugated compared with B100. The surface deposit contour was observed using a digital microscope KH-8700 Hirox series, while the structure of the deposit was assessed via SEM. The microstructure of B100 deposits tended to be smooth, with smaller pores.

On the edge of the deposits as shown in Figure 5, which comprised most of their volume, B0 produced a rough, even surface with small pores, while B100 had a smooth surface, but some sections had large pores. This can be observed from the SEM images below. Visually, B100 was seen to be wet, which could mean that it had material that took longer to evaporate.

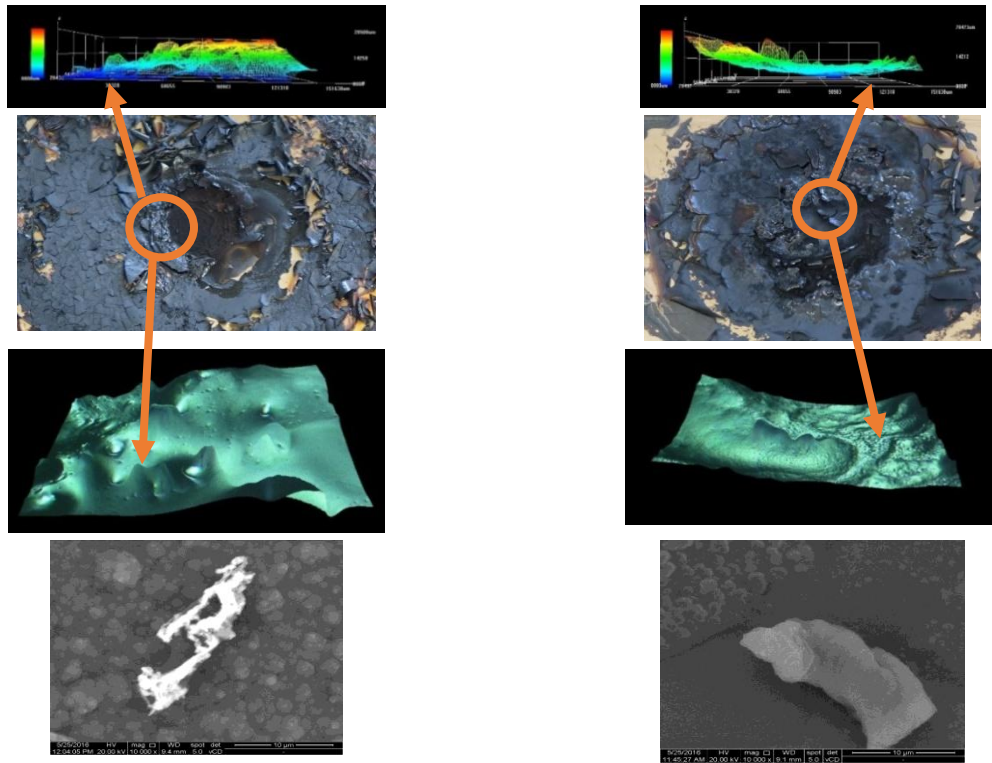


Figure 4 Surface shape and structure of deposits near the core for B0 (left) and B100 (right) at 260°C, with magnification of 500× and 10,000×

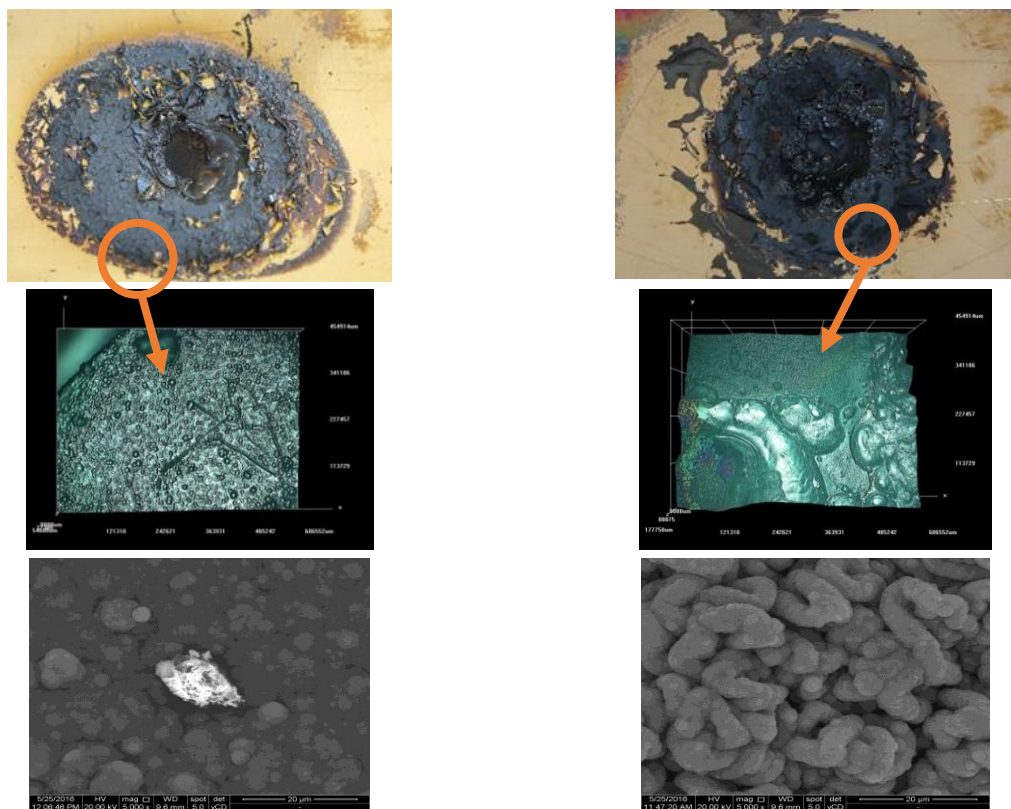


Figure 5 Surface and structure of deposits away from the core for B0 (left) and B100 (right) at 260°C

1378 Deposit Characterization of a Diesel Engine Combustion Chamber by Droplets at Hot Chamber Temperature: Effect of Temperature on Evaporation Time and Deposit Structure

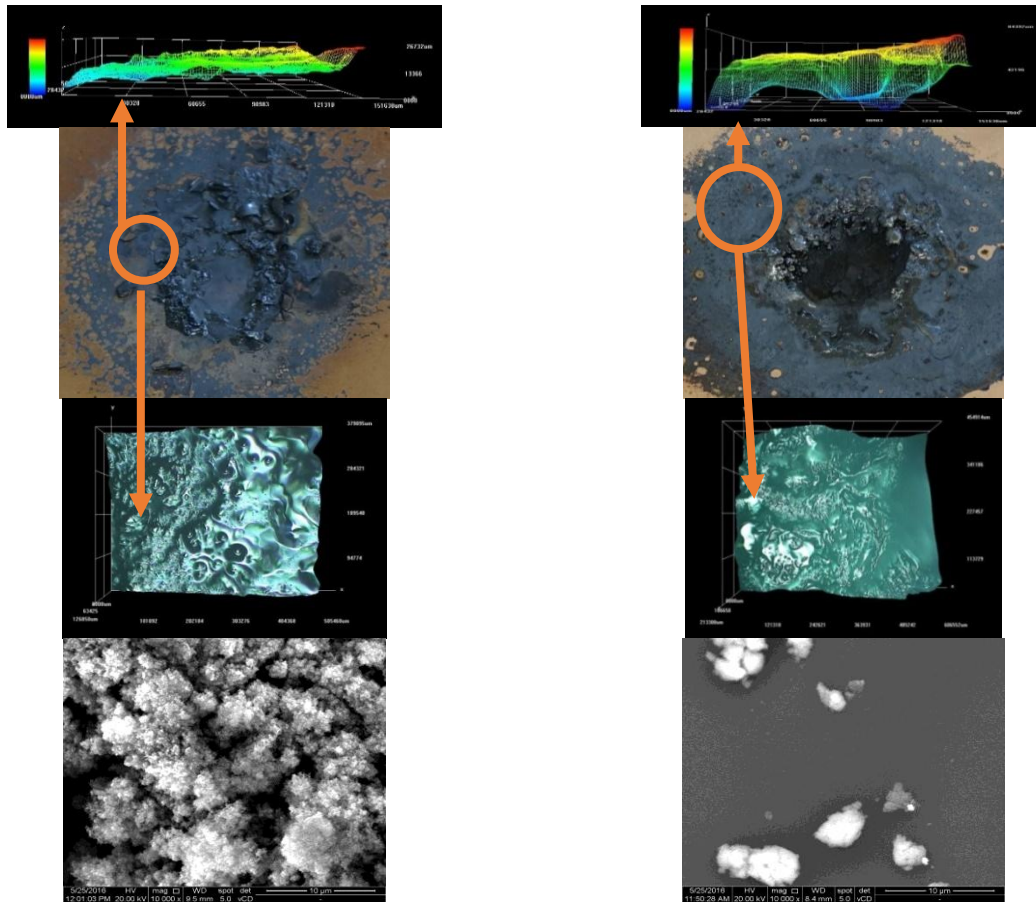


Figure 6 Surface shape and structure of the deposits near the core for B0 (left) and B100 (right) at 300°C

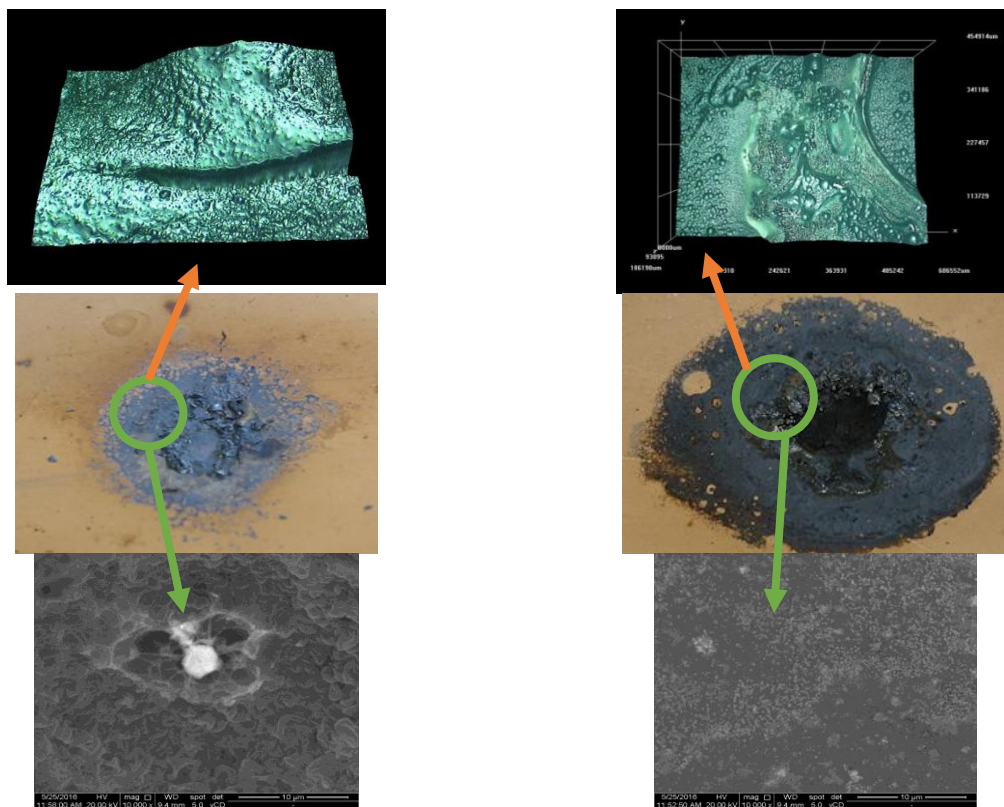


Figure 7 Surface shape and structure of deposits away from the core for B0 (left) and B100 (right) at 300°C

Both close to the core of the droplets and at their side edges as shown in Figures 6 & 7, it could be seen that while the B100 deposits tended to be smooth, they were more porous and wetter than those of B0. At the core of B100, deposits were seen to be higher. There were also fragments deposited on the outer side of the deposits of B0 and B100, comprising dried and volatile material.

At temperatures of 300°C on a smooth part of the deposit, B0 had pores that were larger than those of B100, but of lower intensity. The rough parts of B0 deposits were also more porous. Physically, with increasing temperature, a small porous deposit had more difficulty evaporating. When compared at temperatures of 260°C and 300°C, both fuels narrowed in diameter. Cracked sections at 260°C did not appear at 300°C. The mass was reduced in B0 by 7×, while for B100 this was just 1.7×. Therefore, it can be concluded that the existence of a mass that had a high boiling point in the deposit of B100 hampered the evaporation of such a deposit.

4. CONCLUSION

Based on test data, it was seen that B0 evaporation time was faster than that of B100 at each temperature, to a temperature of MEP. After reaching the MEP temperature, evaporation rates tended to be similar. This was likely due to the B100-forming compounds consisting of long chains that were not easily evaporated. The MEP of B0 occurred at lower temperatures than B100. Evaporation time affected the area and amount of the deposit formed. The faster the evaporation time, the smaller the area of the deposit generated. On B0, the closer the room temperature was to the MEP, the more intense were the pores, but the distribution drastically narrowed. Meanwhile, on B100, the more temperatures neared the MEP, the less pores were produced. Temperatures that rose to near the MEP resulted in hard deposits, while temperatures far below MEP produced wet deposits.

5. REFERENCES

- Arifin, Y.M., Arai, M., 2010. The Effect of Hot Surface Temperature on Diesel Fuel Deposit Formation. *Fuel*, Volume 89(5), pp. 934–942
- Arifin, Y.M., Furuhashi, T., Saito, M., Arai, M., 2008. Diesel and Bio-diesel Fuel Deposits on A Hot Surface. *Fuel*, Volume 87(89), pp. 1601–1609
- Berthiaume, D., Tremblay, A., 2006. *Study of the Rancimat Test Method in Measuring the Oxidation Stability of Biodiesel Ester and Blends*. Quebec, Canada: OLEOTEK, Inc., & Natural Resources
- Chevron, 2007. Diesel Fuels Technical Review. Available online at: <https://www.chevron.com/-/media/chevron/operations/documents/diesel-fuel-tech-review.pdf>
- Fattah, I.M.R., Masjuki, H.H., Kalam, M.A., Hazrat, B.M.M.S., Imtenan, A.M.A., 2014. Effect of Antioxidants on Oxidation Stability of Biodiesel Derived from Vegetable-and Animal-Based Feedstocks. *Renewable and Sustainable Energy Reviews*, Volume 30, pp. 356–370
- Frankel, E.N., 2005. *Lipid Oxidation, edited by P.J. Barnes & Associates (2nd edition)*. Bridgwater, England: The Oily Press
- Lepperhoff, G., Houben, M., 1993. Mechanism of Deposit Formation in Internal Combustion Engines and Heat Exchangers. *SAE Technical Paper 931032*
- Lin, Y.S., Lin, H.P., 2011. Spray Characteristics of Emulsified Castor Biodiesel on Engine Emissions and Deposit Formation. *Renewable Energy*, Volume 36(12), pp. 3507–3516
- Ma'ruf, M., 2015. The Effects of Additives Antioxidant on Biodiesel Deposit Formation, Study on Hot Plate and Diesel. *Graduate Thesis*. Departement of Mechanical Engineering, Faculty of Engineering, Universitas Indonesia

- Munson, B.R., Okiishi T.H., Huebsch, W.W.L., 2009. *Fundamentals of Fluid Mechanics (6th edition)*, John Wiley & Sons, Inc. New Jersey, USA
- Pulkrabek, W.W., 1997. *Engineering Fundamentals of the Internal Combustion Engine*. New Jersey: Prentice Hall
- Tang, H., Wang, A., Salley, S.O., Ng, K.Y.S., 2008. The Effect of Natural and Synthetic Antioxidants on the Oxidative Stability of Biodiesel. *Journal of the American Oil Chemists' Society*, Volume 85(4), pp. 373–382
- Wibowo, E., 2015. *Bioenergy Development in Indonesia*. Directorate Bioenergy, Directorate General of New Renewable Energy and Energy Conservation Indonesia
- Yang, Z., Hollebone, B.P., Wang, Z., Yang, C., Landriault, M., 2013. Factors Affecting Oxidation Stability of Commercially Available Biodiesel Products. *Fuel Processing Technology*, Volume 106, pp. 366–375
- Zhang, H., Xing, J., Guo, C., 2013. Thermal Analysis of Diesel Engine Piston. *Journal of Chemical and Pharmaceutical Research*, Volume 5(9), pp. 388–393

APPENDIX 1

Standard and quality of Indonesian biodiesel (SNI 7182:2012)

No.	Parameter	Requirement	Units (min./max.)	Method
1	Density at Temperature 40 °C	850-890	kg/m ³	ASTM D-1298/D-4052/ see part. 9.1 SNI 7182:21012
2	Kinematic viscosity (Temperature 40 °C)	2.3-6.0	mm ² /s (cSt)	ASTM D-445/ see part. 9.2 SNI 7182:2012
3	Cetane number	51	min.	ASTM D-613/D-6890/ see part. 9.3 SNI 7182:21012
4	Flash point (closed condition) cup	100	°C, min.	ASTM D-93/ see part. 9.4 SNI 7182:21012
5	Cloud point	18	°C, max.	ASTM D-2500/ see part. 9.5 SNI 7182:21012
6	Copper plate corrosion (three hours)	1	-	ASTM D-130/ see part. 9.6 SNI 7182:21012
7	Carbon residue on 10% distillation residue	0.05 0.3	%-mass, max.	ASTM D-4530/D-189/ see part. 9.7 SNI 7182:21012
8	Water and sediment	0.05	%-vol., max.	ASTM D-2709/ see part. 9.8 SNI 7182:21012
9	Distillation temperature 90%	360	°C, max.	ASTM D-1160/ see part. 9.9 SNI 7182:21012
10	Sulfate ash	0.02	%-mass, max.	ASTM D-874/ see part. 9.10 SNI 7182:21012
11	Sulfate	100	mg/kg, max.	ASTM D-5453/D-1266/D-4294/D-2622 see part. 9.11 SNI 7182:21012
12	Phosphor	10	mg/kg, max.	AOCS Ca 12-55/see part. 9.12 SNI 7182:2012
13	Acid number	0.6	mg-KOH/g, max.	AOCS Cd 3d-63/ASTM D-664/see part. 9.13 SNI 7182:2012
14	Free glycerol	0.02	%-mass, max.	AOCS Ca 14-56/ASTM D-6484/see part. 9.14 SNI 7182:2012
15	Total glycerol	0.24	%-mass, max.	AOCS Ca 14-56/ASTM D-6484/see part. 9.14 SNI 7182:2012
16	Methyl ester content	96.5	%-mass, min.	SNI 7182:2012/see part. 9.15 SNI 7182:2012
17	Iodine number	115	%-mass, max. (gr-I ₂ /100 g)	AOCS Cd 1-25/see part. 9.16 SNI 7182:2012
18	Oxidation stability, induction period: Rancimate method	360		EN 15751/see part. 9.17.1 SNI 7182:2012
	Oxidation stability, induction period: Petro-oxy method	27		ASTM D-7545/see part. 9.17 SNI 7182:2012